SAND94-3231C For presentation at the 1995 National Heat Transfer Conference, Portland, Oregon August 5-9, 1995

THE EFFECT OF TRAVEL SPEED ON THERMAL RESPONSE IN CO_2 LASER WELDING OF SMALL ELECTRONIC COMPONENTS

S. E. Gianoulakis
Thermal and Fluid Engineering Department
Sandia National Laboratories
Albuquerque, New Mexico 87185-5800

S. N. Burchett
Engineering and Manufacturing Mechanics Department
Sandia National Laboratories
Albuquerque, New Mexico 87185-5800

P. W. Fuerschbach and G. A. Knorovsky
Physical & Joining Metallurgy Department
Sandia National Laboratories
Albuquerque, New Mexico 87185-5800

This work was supported by the United States Department of Energy under Contract DE-AC04-94AL85000.

ABSTRACT

A comprehensive three-dimensional numerical investigation of the effect of heat source travel speed on temperatures and resulting thermal stresses was performed for CO_2-laser welding. The test specimen was a small thermal battery header containing several stress-sensitive glass-to-metal seals surrounding the electrical connections and a temperature sensitive ignitor located under the header near the center. Predictions of the thermal stresses and temperatures in the battery header were made for several travel speeds of the laser. The travel speeds examined ranged from 10mm/sec to 50mm/sec. The results indicate that faster weld speeds result in lower temperatures and stresses for the same size weld. This is because the higher speed welds are more efficient, requiring less energy to produce a given weld. Less energy absorbed by the workpiece results in lower temperatures, which results in lower stresses.

INTRODUCTION

Hermetic containers are used to package many types of devices used in modern technology. These containers are typically used to provide an environmental barrier which helps ensure long life and reliability of the component being packaged. A closure weld on the package normally provides the hermeticity. When small electronic components containing glass-to-metal seals are closure welded, the resulting thermal stresses developed in the glass are of concern. If these stresses exceed allowable tensile levels, the glass will crack resulting in loss of hermeticity. Closure welding normally occurs near the end of the assembly process and failure of a seal typically dictates that the entire component be scrapped or reworked often at substantial cost to the manufacturer. A thorough understanding of how various welding parameters affect the stresses in the seals is desirable for development of an optimum weld schedule. Without this understanding, a trial and error process with a statistically significant number of test specimens must be used to help guarantee an acceptable weld. This trial and error process has been used successfully in the past; however, as electrical components being welded are becoming smaller and more complex, and testing more expensive, a more fundamental understanding of the coupled thermal-mechanical interactions during the welding process is becoming more necessary than ever.

There are several approaches that can be taken to minimize the possibility of cracking the glass seals. These approaches include designing special weld joint geometries which act to minimize the required heat input, using high power density, low-total heat input welding processes such as laser and electron beam, keeping the seals as far as possible from the weld, and process optimization.

This paper examines one of the variables used for process optimization; laser travel speed. A comprehensive three-dimensional numerical investigation was used to study the effect of heat source travel speed on temperatures and resulting thermal stresses in a small battery header which is being laser welded. The total energy input required for a given size weld is inversely related to the travel speed, but asymptotically approaches a saturation level as the travel speed increases.

COMPUTATIONAL PROCEDURE

The geometry of the thermal battery header and details of the glass-to-metal seals are shown in Figure 1. The materials used for the battery include: 304L stainless steel for the header and case, Corning 9010 for the glass insulators, and Alloy 52 for the pins. The weld used to seal the header to the casing was an edge weld with a minimum ligament thickness equal to the casing thickness (0.40 mm). The weld begins adjacent to one of the seals and proceeds around the header ending with approximately 15 degrees of overlap.

The numerical approach to estimate the stresses and temperatures seen by the battery components was to use a one-way coupled thermal-mechanical analysis. This was accomplished by first

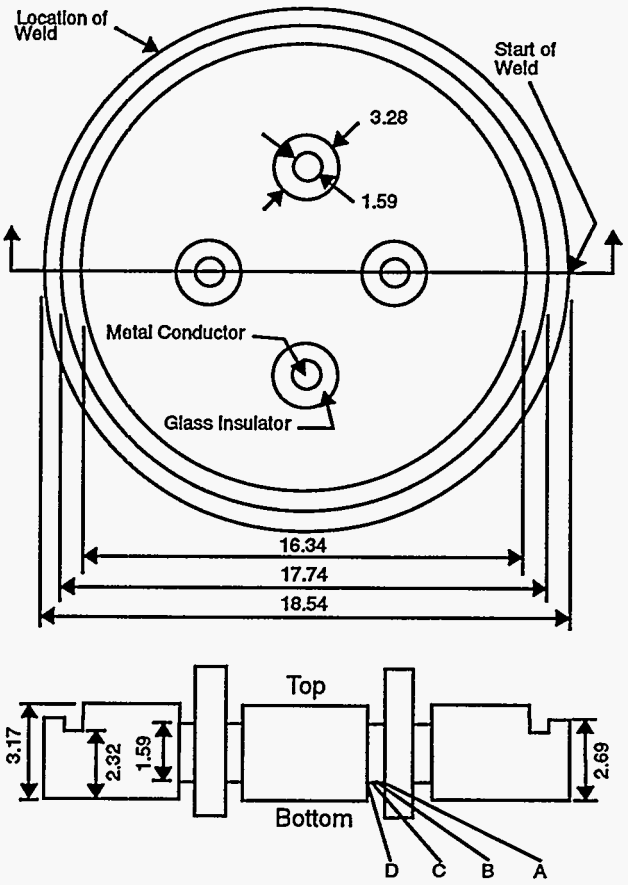

Figure 1: Schematic of Battery Header. Dimensions in mm

performing the transient three-dimensional thermal analysis of the welding process. The temperature histories of the nodes in the thermal mesh were then mapped onto the nodes in the structural mesh and used as source terms to compute the thermally induced stresses. The finite element mesh used for the thermal calculations is shown in Figures 2 and 3. The mesh for the structural calculations was similar with increased mesh densities near the weld, in the header near the seals, and within the seals. A total of 12376 8-node elements were in the thermal mesh and 34950 8-node elements were in the structural mesh. The meshes were generated using P3/PATRAN (PDA Engineering 1993). The thermal calculations were performed using P/THERMAL (PDA Engineering 1993) on a SUN SPARC10-51 workstation. P/THERMAL is a non-linear thermal analysis software package for heat conduction. The structural analyses were performed using JAC3D (Biffle 1993) on a Cray Y-MP. JAC3D is a finite element code for the non-linear quasi-static response of solids using the conjugate gradient method.

The welding heat flux from the laser was simulated by applying trapezoidal-shaped pulses in 15 degree arcs sequentially along the path of the weld. This approach discretely models the continuous laser which is traveling around the battery. 15 degree arcs were chosen for modeling simplicity, and animation of the thermal

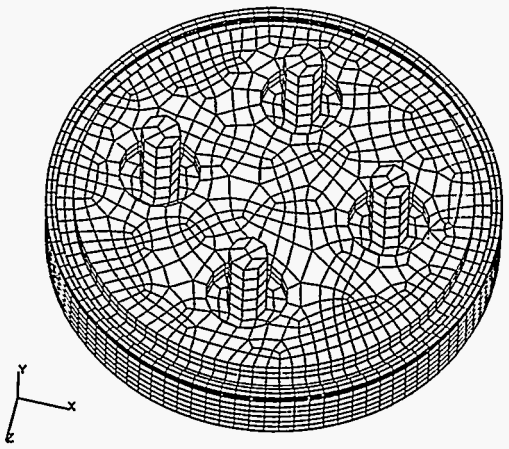

Figure 2: Finite Element Mesh of Battery Header for Thermal Analysis

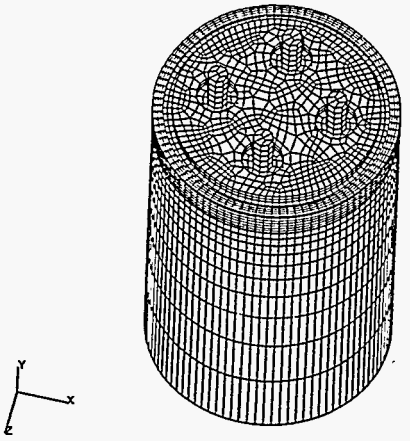

Figure 3: Finite Element Mesh of Battery for Thermal Analysis

results indicated that this discretization was appropriate since the heat source appeared to smoothly travel around the bettery header. Each pulse sequentially turns on and then off to simulate a moving heat source. The ramp time and duration of each pulse was determined based on the travel speed of the laser. The magnitude of the pulses was based on the spot size, energy transfer efficiency, and operating power of the laser. The method to compute the spot size and absorbed laser power to achieve a given size weld will be discussed shortly. The size of the welds for this study was fixed. Figure 4 shows schematically the heat pulses used. Note that the pulses overlap at the midpoint of the ramps. This provides continuity in the rate at which energy is provided to the material, closely representing the actual welding process. The ramp times (both up and down) have durations of 20% of the time that the laser speed in each of the 15 degree arcs along the weld. The dura-

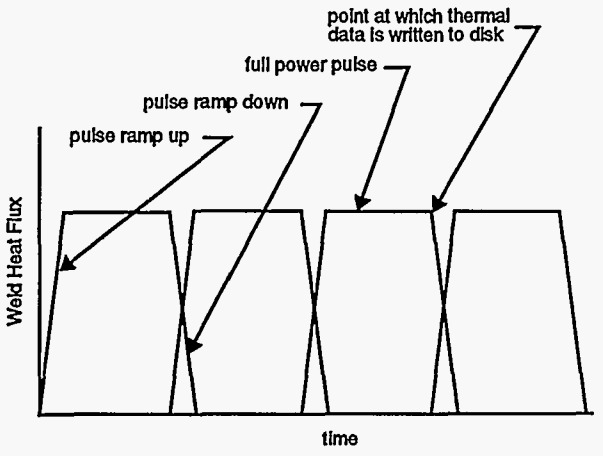

Figure 4: Energy Pulses to Simulate Moving Laser

tion that the pulse is at full power is 80% of the time that the laser spend in each arc. This scheme results in the proper amount of energy (Joules) being deposited in each arc. The total heat input to the material consisted of 24 pulses plus one extra pulse to simulate an overlap region.

Material properties for the stainless steel header and casing were obtained from (Touloukian 1972) and input as functions of temperature. To model the latent heat of fusion and vaporization, a step change in the specific heat was included over the transition regions between solid and liquid, and liquid and vapor respectively. The material properties for the Alloy 52 pins and Corning 9010 glass insulators were obtained from vendor literature.

The boundary conditions in the thermal model included natural convection and radiation to the surroundings. Since the purpose of this study was to examine the effect of travel speed on temperature and stresses, detailed convection and radiation models were not used. Rather, simple convection correlations for vertical surfaces (Incopera and Dewitt 1990) and gray body radiation relations (Siegel and Howell 1981) were included.

The temperature history data provided to the structural code was saved to disk once per pulse during the weld and then at a reduced frequency during the cooldown period following the weld. The times at which the temperature data are written to disk correspond to when the pulse just begins to ramp down. Refer to Figure 4 for where this occurs in each pulse.

During the fabrication of headers containing glass-to-metal seals, stresses can be generated in the glass insulators, metal electrical connector pins, and the metal housing during the glassing operation due to differential thermal contraction of the glass and metal as the assembly cools to room temperature. Two design approaches are used to control the tensile stresses generated in the glass. One approach is to use glass and metal materials that have nearly the same thermal expansion properties. This approach, referred to as a matched seal, produces a relatively stress-free state in the assembly after manufacture. The second approach is to use a glass that has a thermal expansion coefficient that is less than the thermal expansion coefficient of the header. This seal is called a compression seal because the glass near the housing is compressed during cooling. Design guidelines for coaxial compression pin seals have been developed (Miller and Burchett, 1982) to minimize any tensile stress in the glass of a compression pin seal, thus enhancing the survivability of glass in subsequent manufacturing or use environments. In this study, the material combination produces a compression pin seal. Therefore, the room temperature residual stress must be determined prior to the laser weld simulation. This was accomplished by modifying the laser weld temperature history to include an initial stress-free temperature at the set-point temperature of the glass (445 °C) and uniformly cooling to room temperature (27 °C). The stresses in the assembly were then computed for both the manufacturing glassing operation and the subsequent laser weld operation.

Room temperature material properties used in these analyses are given in Table 1. The glass was assumed to remain linear elastic below its set-point temperature. The metals were modeled as temperature dependent strain hardening elastic-plastic materials. At zones where the material exceeded the melt temperature, the deviatoric stresses were set to zero and the history state variables were reset to zero. As the temperatures in these elements cooled below melt, the stresses were once again developed.

Table 1: Room Temperature Mechanical Properties

Material	Young's Modulus GPa	Poisson's Ratio	Yield Strength MPa	Thermal Expansion 1/C
Alloy 52 Pin	206.9	0.3	344.8	10.2E-6
9010 Glass	67.6	0.21	NA	10.2E-6
304SS Housing	193.1	0.27	207.0	18.4E-6

WELD SCHEDULE DETERMINATION

Melting efficiency is a figure of merit for fusion welding which indicates how effectively the heat deposited into the workpiece is utilized. Melting efficiency (η_m) is the ratio of the heat necessary to just melt the fusion zone to the heat absorbed by the workpiece. It is calculated by dividing the enthalpy of the weld volume (δhV where V is the weld volume) by the net heat input (Q_i) as given by the following expression:

$$\eta_m = \frac{V\delta h}{Q_i} \qquad 1$$

The enthalpy of the weld volume is determined by multiplying the weld volume by the enthalpy change required to bring a unit volume of the metal from room temperature (T_r) to the liquidus

temperature (T_l). It is given by the following expression where c_p is the specific heat and Δh_f is the heat of fusion :

$$\delta h = \Delta h_f + \int_{T_r}^{T_l} c_p(T)\, dT \qquad 2$$

It is important to note that it is possible to produce welds that are equivalent in size and geometry but have unlike overall heat inputs and thermal histories because of variation in melting efficiency.

To compare welds with varying melting efficiencies, a mathematical model for laser welding (Fuerschbach 1994) was employed. The weld penetration depth was also fixed and was determined using empirical correlations that relate penetration to laser beam irradiance and travel speed. The model uses dimensionless parameters that relate the cross sectional area of a laser weld to the travel speed and the net heat absorbed by the workpiece. The melting efficiency is directly calculated from the ratio of the two dimensionless parameters. The weld parameters selected to produce welds of equivalent size but with varying melting efficiencies are given in Table 2. These five weld schedules were analyzed to examine how melting efficiency affects the temperature fields. Three of these weld schedules were further analyzed to examine stresses produced in the glass seals.

Table 2: Weld Schedules

Travel Speed [mm/sec]	Absorbed Laser Power [W]	Melting Efficiency
10	230	0.12
20	240	0.25
30	325	0.34
40	325	0.39
50	375	0.41

RESULTS AND DISCUSSION

Figure 5 shows the temperature histories of the ignitor located in the center of the bottom side of the battery header. The maximum temperatures exhibited by the ignitor are 142.2, 91.4, 79.2, 74.4, and 72.0 °C for laser travel speeds of 10, 20, 30, 40, and 50 mm/sec respectively. These temperatures decrease with increasing laser travel speeds. The weld schedules with higher travel speeds are more efficient. Less overall energy is required to produce a weld of given size. Therefore, less energy goes into heating of the bulk material away from the weld, resulting in lower temperatures at the ignitor. Figure 6, 7, and 8 show contours (same scale) of the temperature field for three of the five weld schedules examined after one revolution of the laser. The times associated with these plots are 5.73 second, 1.91 second, and 1.14 second for laser travel speeds of 10 mm/sec, 30 mm/sec, and 50 mm/sec. respectively. These figures clearly show that as the travel speed

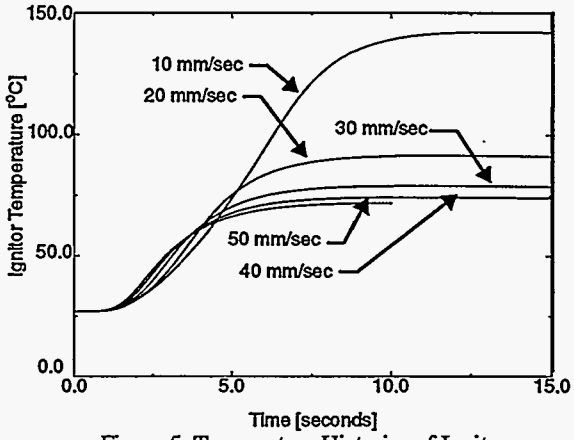

Figure 5: Temperature Histories of Ignitor

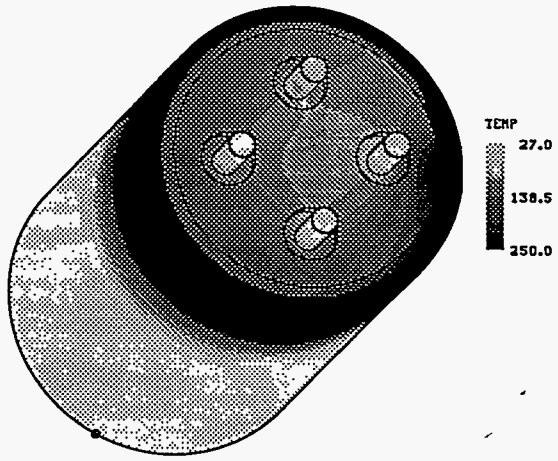

Figure 6: Temperature Contours [°C] After One Revolution 10 mm/sec

increases, the isotherms become more concentric and the body temperatures are reduced.

Three of the five weld schedules (10 mm/sec, 30 mm/sec, and 50mm/sec) were additionally analyzed to examine how the laser travel speed affected the transient thermal stresses in the glass insulators. The interpretation of the results is complicated by the non-uniform initial residual stresses developed in the glass seal due to glassing. Additionally, the thermal stresses in the headers are in excess of the yield strength of 304SS at regions around the glass insulators, therefore the numerical solution is nonlinear. The most detrimental stress change in the glass due to welding occurs on the bottom surface of the glass insulator that is next to the start/stop location of the laser heat source as the heat source is completing the weld (one revolution). Figures 9-12 compare the maximum principal stress-time histories for three travel speeds at four locations through the glass section starting from the inside surface next to the pin (point A) to the outside surface next to the housing (point D), respectively. See Figure 1 for locations of points A

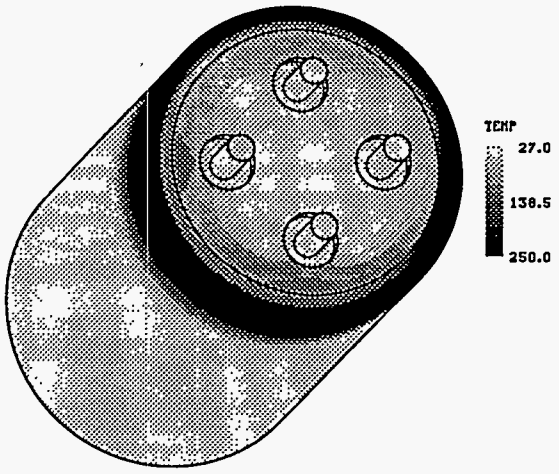

Figure 7: Temperature Contours [°C] After One Revolution 30mm/sec

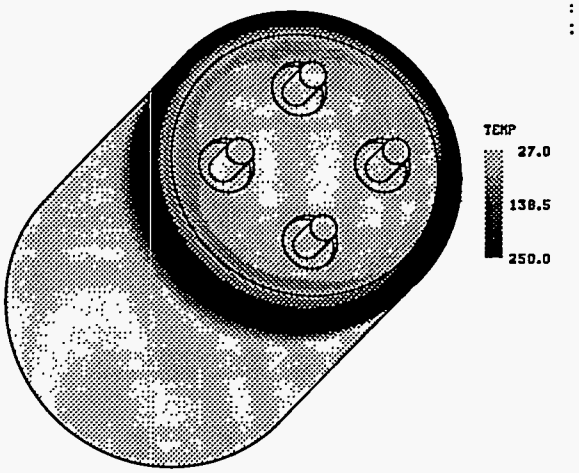

Figure 8: Temperature Contours [°C] After One Revolution 50 mm/sec

through D. The results are normalized with time, therefore normalized time 0.0 corresponds to the start of the weld process and normalized time 1.0 corresponds to one complete revolution of the laser. The stresses at normalized time 0.0 are residual stresses due to glassing. These results indicate that some tensile stresses are developed in portions of the glass insulator, particularly at point C, due to manufacturing. This may indicate that the geometric design of the coaxial pin seal is not optimum. The transient stress results clearly indicate that as the travel speed increases, detrimental stress changes in the glass are minimized. For the slowest travel speed evaluated (10mm/sec), detrimental transient tensile stresses are developed in the glass. This weld process travel speed is marginal with increased probability of the glass insulator cracking.

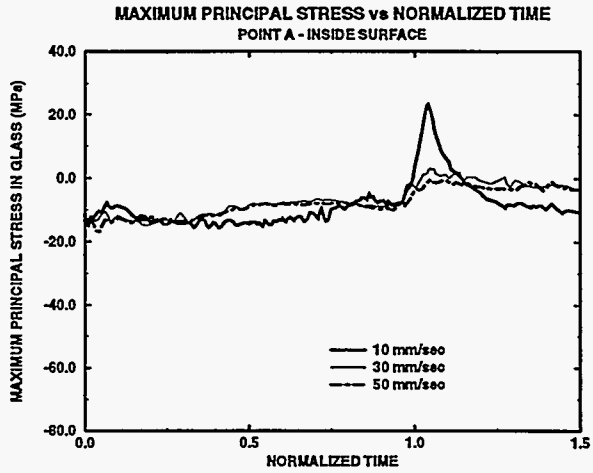

Figure 9: Maximum Principal Stress in Glass @ Point A

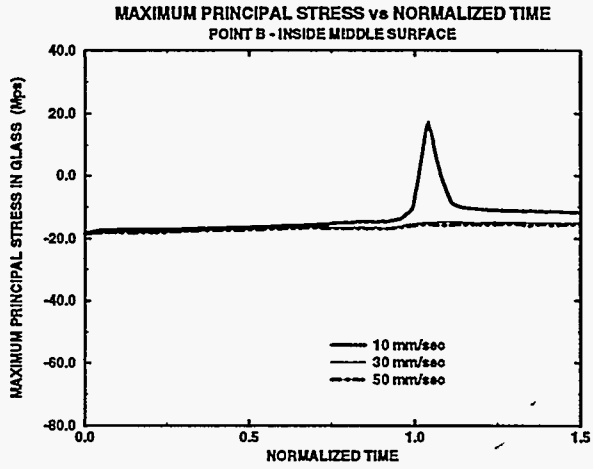

Figure 10: Maximum Principal Stress in Glass @ Point B

CONCLUSIONS

This paper presents a comprehensive three-dimensional numerical investigation of the effect of heat source travel speed on temperatures and resulting thermal stresses for CO_2-laser welding. It was initially postulated that if the laser energy was deposited faster (faster travel speeds) the result could be higher thermal stresses due to higher thermal gradients. This paper shows, however that for a constant weld size, lower temperatures and stresses result for the faster travel speed welds since the process is more efficient. requiring less energy to produce a given weld. Less energy absorbed by the workpiece results in lower temperatures, which results in lower stresses.The results indicate that for a travel speed of 10 mm/sec, additional detrimental transient stresses are developed in the glass seals. In this paper, a "compression" pin seal was chosen for investigation. If a "matched" seal was evalu-

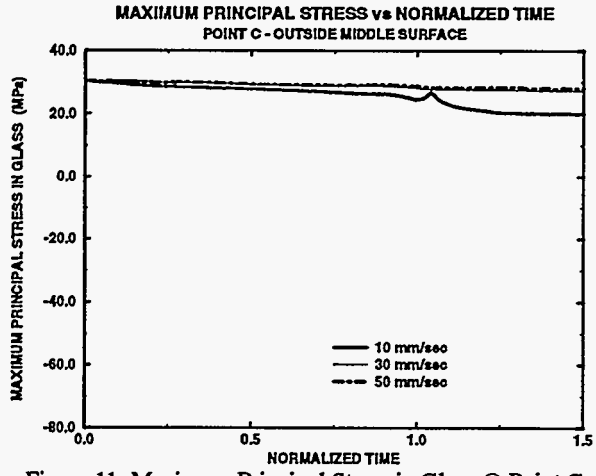

Figure 11: Maximum Principal Stress in Glass @ Point C

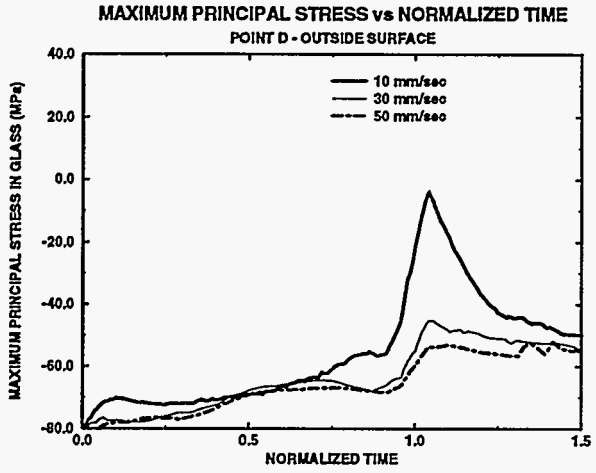

Figure 12: Maximum Principal Stress in Glass @ Point D

ated, the transient thermal stresses may be much more detrimental since the initial compression does not need to be overcome.

Biffle, J. H., 1993 "JAC3D - A Three Dimensional FInite Element Computer Code for the Non-Linear Quasi-Static Response of Solids with the Conjugate Gradient Method," SAND87-1305, Sandia National Laboratories.

Fuerschbach, P. W., "Measurement and Prediction of Energy Transfer Efficiency in Laser Beam Welding," submitted for publication in *Welding Journal.*

Incopera, F. P. and Dewitt, D. P., 1990, *Fundamentals of Heat and Mass Transfer*, 3rd edition, John Wiley and Sons, pp. 541-554.

Miller, J. D. and Burchett, S. N., 1982 "Some Guidelines for the mechanical Design of Coaxial Compression Seals," SAND82-0057, Sandia National Laboratories.

PDA Engineering, 1993 "P3/PATRAN Users Manual," Costa Mesa CA.

PDA Engineering, 1993 "P/THERMAL Users Manual," Costa Mesa CA.

Siegel, R. and Howell, J. R., 1981, *Thermal Radiation Heat Transfer,* 2nd edition, Hemisphere, pp. 236-246.

Touloukian, Y. S. and Ho, C. Y., 1972, *Thermophysical Properties of Matter*, Plenum Press.